SECURITY CLASSIFICATION OF THIS PAGE (When Data Entered)

# REPORT DOCUMENTATION PAGE

READ INSTRUCTIONS BEFORE COMPLETING FORM

| | |
|---|---|
| 1. REPORT NUMBER: AMRL-TR-78-99 | 2. GOVT ACCESSION NO. |
| 3. RECIPIENT'S CATALOG NUMBER | |
| 4. TITLE (and Subtitle): PROCEDURES USED TO GENERATE INPUT DATA SETS FOR THE ARTICULATED TOTAL BODY MODEL FROM ANTHROPOMETRIC DATA, | 5. TYPE OF REPORT & PERIOD COVERED: PRESENTATION |
| | 6. PERFORMING ORG. REPORT NUMBER |
| 7. AUTHOR(s): DUANE G. LEET | 8. CONTRACT OR GRANT NUMBER(s): F33615-78-C-0504 |
| 9. PERFORMING ORGANIZATION NAME AND ADDRESS: UNIVERSITY OF DAYTON RESEARCH INSTITUTE, 300 COLLEGE PARK, DAYTON, OHIO 45469 105 400 | 10. PROGRAM ELEMENT, PROJECT, TASK AREA & WORK UNIT NUMBERS: 62202F ; 7231-05-18 05 |
| 11. CONTROLLING OFFICE NAME AND ADDRESS: Aerospace Medical Research Laboratory, Aerospace Medical Division, Air Force Systems Command, Wright-Patterson Air Force Base, Ohio 45433 | 12. REPORT DATE: SEPTEMBER 1978 |
| | 13. NUMBER OF PAGES: 50 |
| 14. MONITORING AGENCY NAME & ADDRESS (if different from Controlling Office) | 15. SECURITY CLASS. (of this report): UNCLASSIFIED |
| | 15a. DECLASSIFICATION/DOWNGRADING SCHEDULE |

LEVEL II

16. DISTRIBUTION STATEMENT (of this Report)

58 p.

Approved for release to the public; distribution unlimited



17. DISTRIBUTION STATEMENT (of the abstract entered in Block 20, if different from Report)

18. SUPPLEMENTARY NOTES

Prepared and presented at Specialist' Aerospace Medical Panel Meeting (NATO/AGARD) in Paris France, 6-10 November 1978

19. KEY WORDS (Continue on reverse side if necessary and identify by block number)

INERTIA PROPERTIES
CONTACT ELLIPSOID DIMENSIONS
JOINT LOCATIONS
VARIOUS JOINT STIFFNESS

20. ABSTRACT (Continue on reverse side if necessary and identify by block number)

DD FORM 1 JAN 73 1473 EDITION OF 1 NOV 65 IS OBSOLETE

105 400

SECURITY CLASSIFICATION OF THIS PAGE (When Data Entered)

# SECTION 1
# INTRODUCTION

Protection of passengers from injury during vehicle and aircraft crashes and the protection of a crew from injury during aircraft ejection situations is one of the important design objectives of vehicle and aircraft design engineers. An increasingly important tool in evaluating the safety aspects of different designs is computer software simulation. Calspan Corporation has developed a particularly sophisticated class of these programs. The class includes the 3-D Crash Victim Simulator (CVS) Model, developed under DOT sponsorship (Fleck, et al, 1974), and the Articulated Total Body (ATB) Model, developed from the CVS Model under the sponsorship of the U.S. Air Force Aerospace Medical Research Laboratories (AMRL) specifically for application to aerospace-type problems (Fleck and Butler, 1975). These programs model the human (or laboratory animal) body as a multi-segment chained system. Currently 15 segments are defined: head, neck, upper arm (left and right), lower arm (left and right; includes the hand), upper torso (thoracic region), middle torso (viscera), lower torso (pelvic region), upper leg (left and right), lower leg (left and right), and foot (left and right). Figure 1 provides two views of a body on which standard body segment cut-planes have been marked. The actual body landmarks defining these cut-planes are described in Chandler, et al (1975).

Among the input data required on each segment are:

- inertia properties (mass, center of mass, principal moments, principal axes orientation)
- contact ellipsoid dimensions, axes origin with respect to the center of mass, and axes orientation with respect to the principal axes

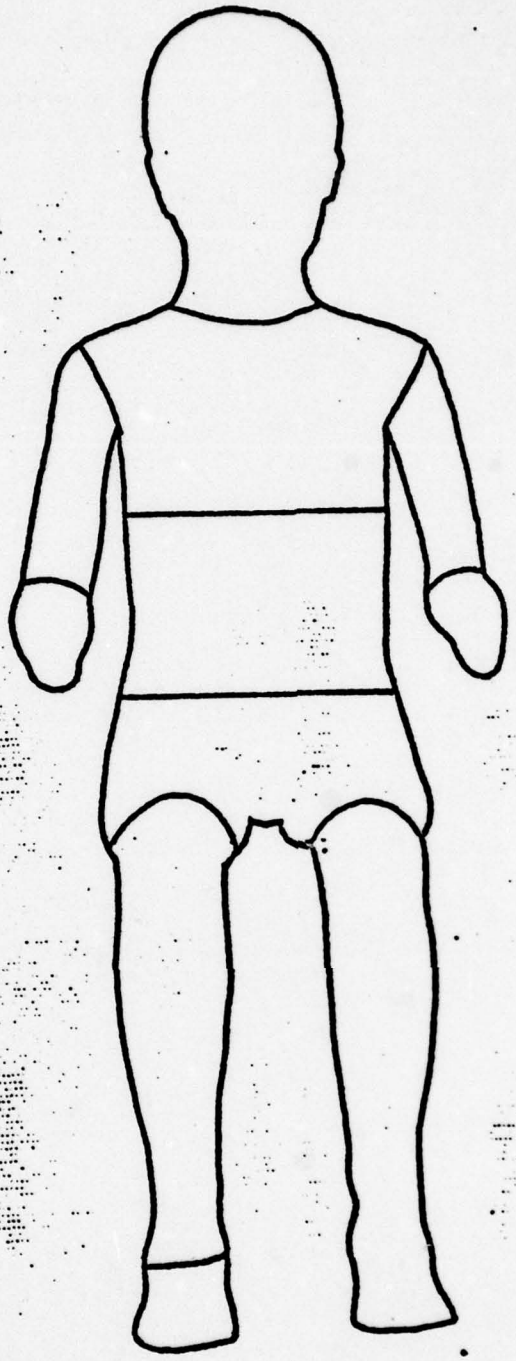



**Figure 1a.** The Fifteen Body Segments Marked on Front View of a Six-Year-Old Child Manikin Developed From Anthropometric Data By Young, et al (1976).

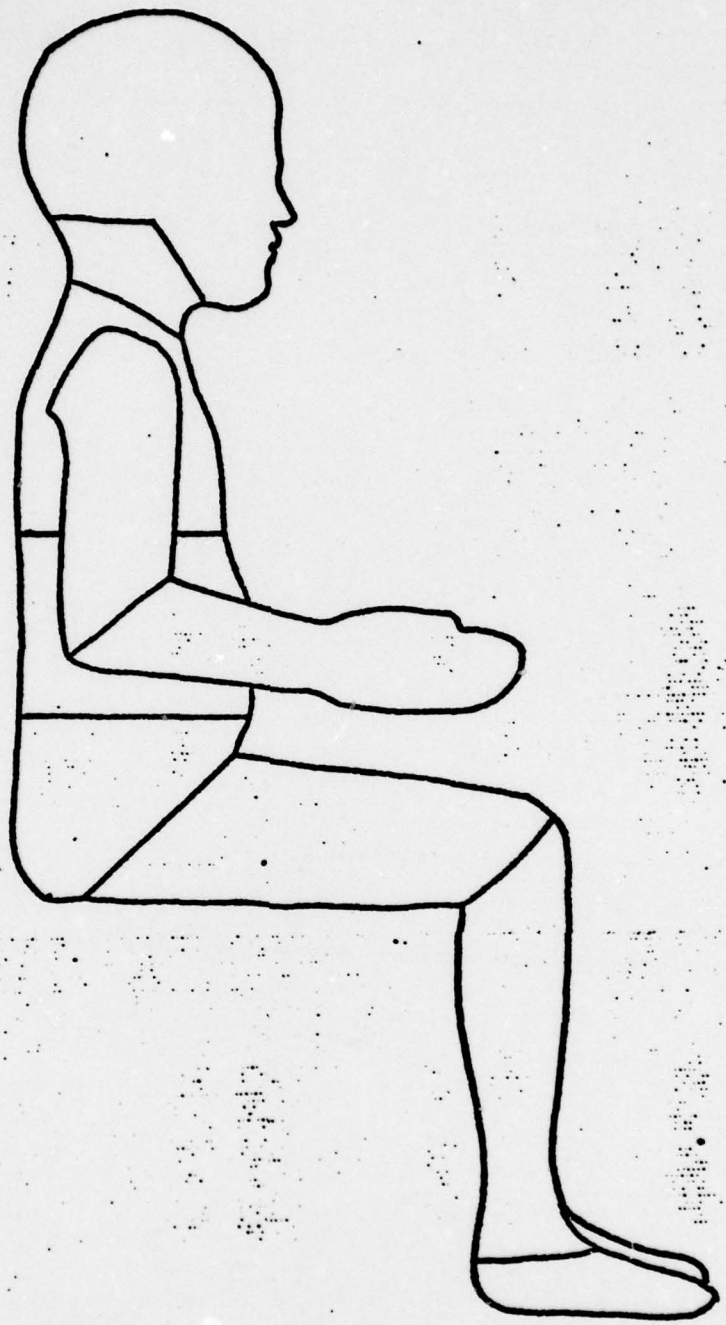

Figure 1b. The Fifteen Body Segments Marked on Right Side View of a Six-Year-Old Child Manikin Developed From Anthropometric Data By Young, et al (1976).

- joint locations with respect to the center of mass, and joint axes orientation (Each joint has two sets of axes, one for each segment associated with the joint. These axes are used to define torques at the joint.)
- various joint stiffness and friction constants

In addition, data must be supplied to define the initial orientation of the body with respect to an external reference coordinate system. The environment (contact planes, restraint systems) must also be defined, as well as remaining initial conditions and the external stimuli to be applied to the system.

The program simulates the dynamics of body motion using a unique method that has been shown to be equivalent to the Lagrange method. Motion picture films of the dynamics can be produced through the use of plot packages supplied with the simulation program. The quality of the simulation is demonstrated in the paper in this session by Ints Kaleps.

The University of Dayton Research Institute, under the sponsorship of AMRL, is currently involved in a research program to develop input data sets for the ATB Model program. The next four sections of this paper provide a general background for the techniques we have developed to generate these input data sets from anthropometric data. The final section discusses the current state-of-the-art in implementing these techniques. The appendices provide some details on the techniques that have been developed.

## SECTION 2

## TECHNIQUES USED TO GENERATE BODY SEGMENT INERTIAL DATA

There are two basic approaches used to obtain body segment inertial data. One approach is to perform actual pendulum-type measurements on cadaveric body segments. There have been only two significant studies performed in the U.S. on human cadavers using this approach, one by Chandler, et al (1975), which included data on all the body segments of six adult male cadavers, and the other by Walker, et al (1973), which emphasized the head and neck segments of 20 adult male cadavers. The second approach is to construct a geometric model of a body segment and compute the model's inertial properties. Data used to construct the models are from one of two sources: anthropometric or biostereometric measurements. We will be emphasizing techniques for constructing the geometric models from anthropometric data.

Previous body segment geometric models have been homogeneous ellipsoids, cylinders, or frustrums of circular cones. [See, for example, Reynolds ( ).] We have developed the mathematics for a more general geometric shape shown in Figure 2. This segment model can have up to three parts. One of these parts is the right elliptical solid, which has these characteristics:

- It has two parallel elliptical end-planes. A z-axis is defined through the centroids of these end-planes and is normal to both planes.
- The end-planes and any other cross-section parallel to them are ellipses with centers on the z-axis and semi-axes in the xz- or yz-planes.

For our purposes, the shapes of the right elliptical solid is further restricted to those that can be defined by supplying the semiaxis values of the end-planes and a single cross-section somewhere between the end-planes. Although the other geometric models mentioned have the advantage of having existing closed-form

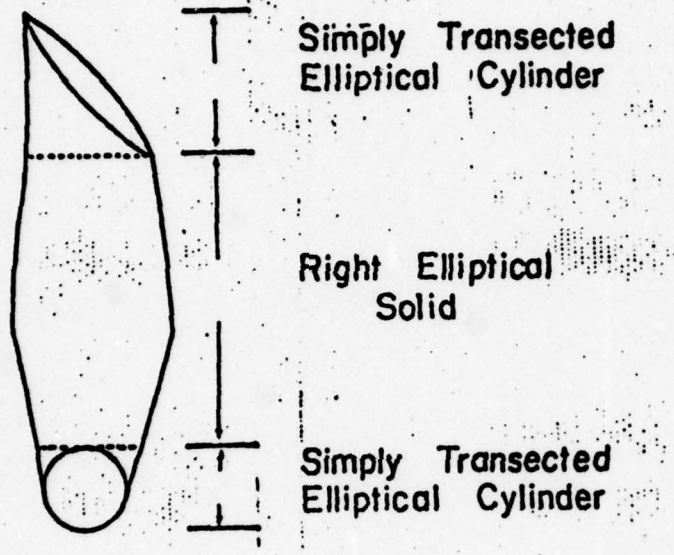


Figure 2. The General Geometric Model.

expressions for their inertial properties, they are relatively poor approximations to actual body segment shapes when compared to the right elliptical solids described here.

The other parts of the segment model in Figure 2 are homogeneous simply-transected elliptical cyclinders. A simply-transected elliptical cylinder is an elliptical cylinder that has been cut diagonally from the edge of one end-plane to the opposite edge of the other end-plane. In addition, if a coordinate system is defined with the z-axis passing through the centroids of the end planes, the cut-plane is parallel to either the x-axis or the y-axis. In the segment model there can be one simply-transected elliptical cylinder at each end of the right elliptical solid.

To complete the specification of our body segment geometric model, we require that the z-axes of the three parts coincide and their xz- and yz-planes must line-up, although they need not coincide. (For example, the xz-plane of a simply-transected elliptical cylinder can line-up with the yz-plane of the right elliptical solid.)

The basic procedure for computing the inertial properties of a body segment using this model is:

1. Select one of the following models:
   a. Right elliptical solid
   b. Simply-transected elliptical cylinder
   c. Right elliptical solid with a simply-transected elliptical cylinder at one end
   d. Right elliptical solid with simply-transected elliptical cylinders at each end
2. Define the local coordinate system for each part and a coordinate system for the segment model as a whole.
3. If the model includes a right elliptical solid:
   a. Identify the proximal, mid, and distal planes
   b. Determine the semiaxes for these planes and the distances between them

c. Determine the density

d. Run the program MISEC2

4. For each simply-transected elliptical cylinder:

   a. Determine the base semiaxes and height

   b. Run the program "Simply-Transected Elliptical Cylinders."

5. Combine the individual segment inertia properties using the program "Parallel Axis Theorem."

6. Obtain the segment principal moments and direction cosine matrix using an available eigenvalue and eigenvector program.

Step 2 requires that local coordinate systems be defined for each part of the segment. It is helpful to orient the segment to the rest of the body by defining proximal and distal ends for the segment as a whole and for each of its parts, with the distal end being furthest from the head. Assuming each part has a proximal end-plane, the origins of the local coordinate systems can be located at the proximal end-plane centroids; otherwise, the origin can be located at the distal end-plane centroid. By convention, the orientation of a segment's positive z-axis is along the cylindrical axis, from the proximal end to the distal end. The positive orientation of a segment's y-axis should be right lateral (out the right side). It follows that the positive orientation of a segment's x-axis should be anterior (out the front).

The MISEC2 program in Step 3d is a very fast interactive FORTRAN program written to compute the inertia properties of the homogeneous right elliptical solid (Leet, 1978a). The program approximates the solid as a stack of elliptical cylinders of varying semiaxis values, computes the inertia properties of each cylinder, computes the center of mass of the solid as a whole, and then used the parallel axis theorem to shift the individual cylinder's center of rotation to the solid's center of mass, where they are appropriately summed to provide the solid's moments of inertia about its center of mass.

The closed-form expressions for the inertial properties of a simply-transected elliptical cylinder, developed in Leet (1978b), are summarized in Appendix B. A convenient HP-97 Calculator program "Simply-Transected Elliptical Cylinders" has been written that computes these properties with respect to various axis orientations.

The HP-97 program "Parallel Axis Theorem" mentioned in Step 5 has been documented in Leet (1978d).

Appendix A specifies the anthropometric data required for each of the body segments in order to use the above procedure.

The *head and neck body segments* are special shapes and we have developed special procedures for them. Previously, the geometric model used for the head was either a homogeneous sphere or ellipsoid. Anthropometric measurements were made of the head's length, width, and depth, and an approximate ellipsoid defined. Then the principal moments were computed from the closed-form expressions. The principal axes are naturally coincident with the geometric axes.

We have developed a novel procedure to obtain the head's principal moments of inertia and principal axes. This procedure is outlined in the following steps:

1. Determine these head measurements:
   a. Head length. (measured from the middle of the forehead[1], just above the eyebrows, to the middle of the back of the head)
   b. Head breadth. (the maximum breadth of the head)
   c. Head height. (the distance from the chin to the top of the head, in a vertical direction)
   d. Mass. (Homogeneity is still assumed.)

[1]Precise anthropometric terminology exists for all locations mentioned; it can be obtained from the author. It is felt that more common, albeit less precise, terminology is more appropriate for this paper.

2. Obtain a direction cosine matrix defining the principal axes orientation with respect to a standard local axis system, and the coefficients of the linear equations relating the principal moments computed from the ellipsoid model to the true principal moment values.

3. Use the program "Moments of Inertia of a Rotated Ellipsoid" to compute the principal moments of the head.

The mass in Step 1 can be determined by obtaining the volume value obtained by emersion and multiplying it by a density representative of the class of humans being modeled. For example, Chandler, et al (1975) have determine that the average density for the head segments of six adult male cadavers was 1.056 (SD = .020).

The direction cosine matrix mentioned in Step 2, which defines the orientation of the principal axes, has been determined for the adult male from the Chandler data (Leet, 1978c). This matrix is

$$\begin{bmatrix} 0.6484 & 0.0000 & -0.7613 \\ 0.0000 & 1.0000 & 0.0000 \\ 0.7613 & 0.0000 & 0.6484 \end{bmatrix}$$

The standard local reference system used has its origin at the head's center of mass, with the positive x-axis in the forward direction (It exits the head at about a point midway between the eyes at the level of the eyebrows.), positive y-axis to the right, and positive z-axis straight down, all with the head level and eyes straight ahead. (The technical terminology is "head oriented in the Frankfort Plane.") The direction cosine matrix specifies that the principal x-axis is rotated 49.6° counterclockwise about the local reference y-axis: this axis exits the head at about the top of the forehead. (The temptation was to say at the hairline, but that, unfortunately, can be too misleading.) The positive principal z-axis, therefore, exits the head approximately through the mouth.

The "Moments of Inertia of a Rotated Ellipsoid" program, which is documented in Leet (1978c), uses the three specified head dimensions to define an ellipsoid whose axes are oriented parallel to the local reference axes and centered at the geometric center of the head. It then uses the direction cosine matrix to define a new ellipsoid whose axes are centered at the geometric center, but oriented parallel to the principal axes. The semiaxis lengths for this ellipsoid are taken as the distances from the origins to the intersection of the principal axes with the first ellipsoid. The principal moments of the new ellipsoid are then calculated.

The principal moments obtained by applying this procedure to the six cadaver heads of the Chandler data were linearly correlated with the empirically determined principal moments. There was a high degree of correlation as can be seen in Figures 3 through 5, with the equations being:

$$I^*_{xx} = 1.98\ I_{axx} - 82.99 \qquad (r^2 = 0.99)$$

$$I^*_{yy} = 1.52\ I_{ayy} - 77.66 \qquad (r^2 = 0.99)$$

$$I^*_{zz} = 1.16\ I_{azz} - 24.22 \qquad (r^2 = 0.92)$$

(The experimentally determined moments are I* and the computed moments are $I_a$.) It is the coefficients of these equations that are referred to in Step 2. The "Moments of Inertia of a Rotated Ellipsoid" program has the capability of performing these linear transformations.

The only inertia property of the head not yet discussed is the center of mass. At present we know of no technique for determining the center of mass of the head from anthropometric data. Edward Becker (1973), at the Naval Aerospace Medical Research Laboratory, has shown that for adult male cadavers, at least, there is only a relatively small variability in the location of the head's center of mass about a mean value of 13 mm in the +x-direction and 21 mm in the -z-direction from the ear hole and midway between the ears.

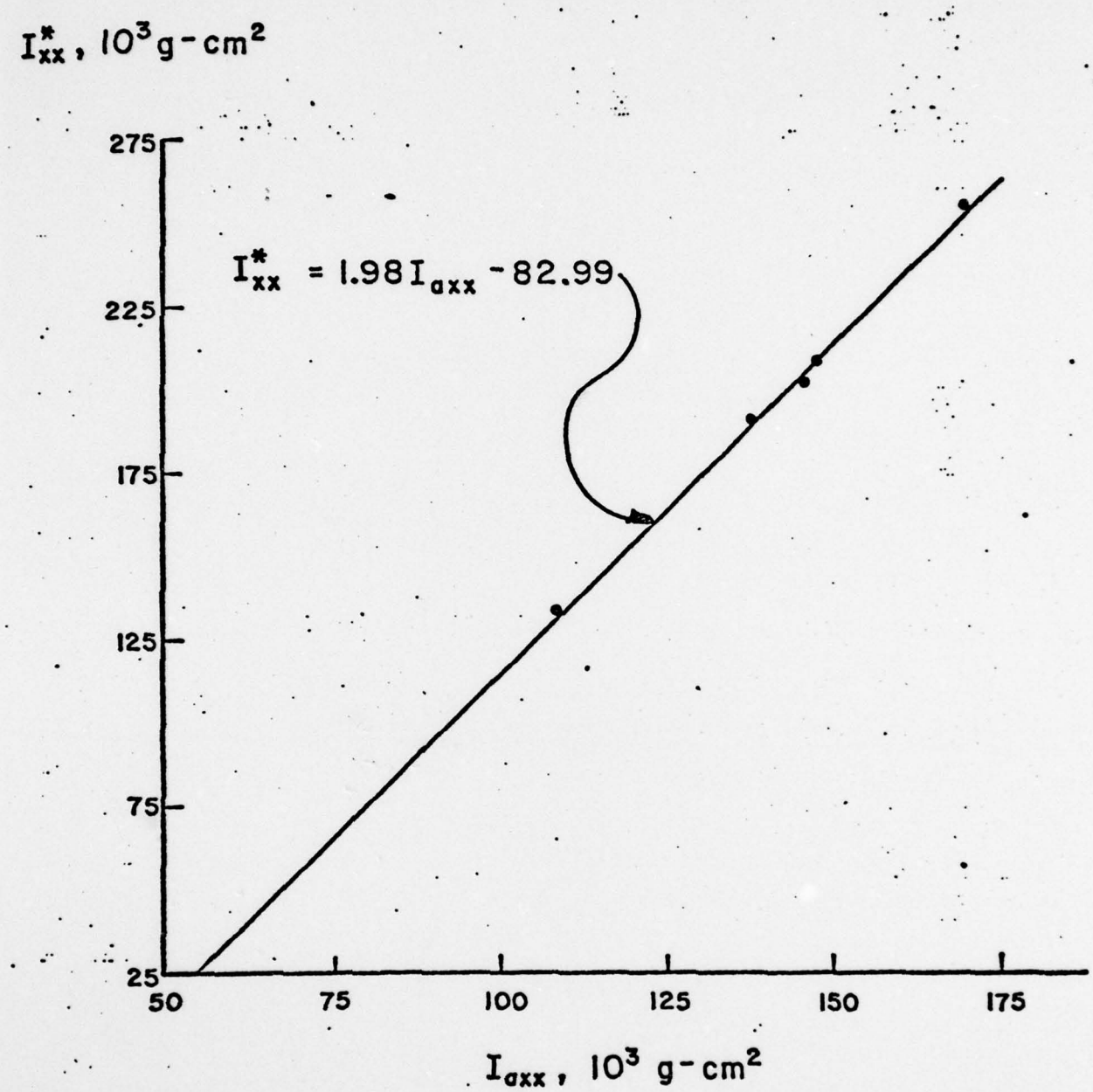


Figure 3. The Head's $I_{axx}$ Principal Moment, Computed Using Rotated Ellipsoid Geometric Model, Compared to the Experimentally Determined Principal Moment, $I^*_{xx}$.

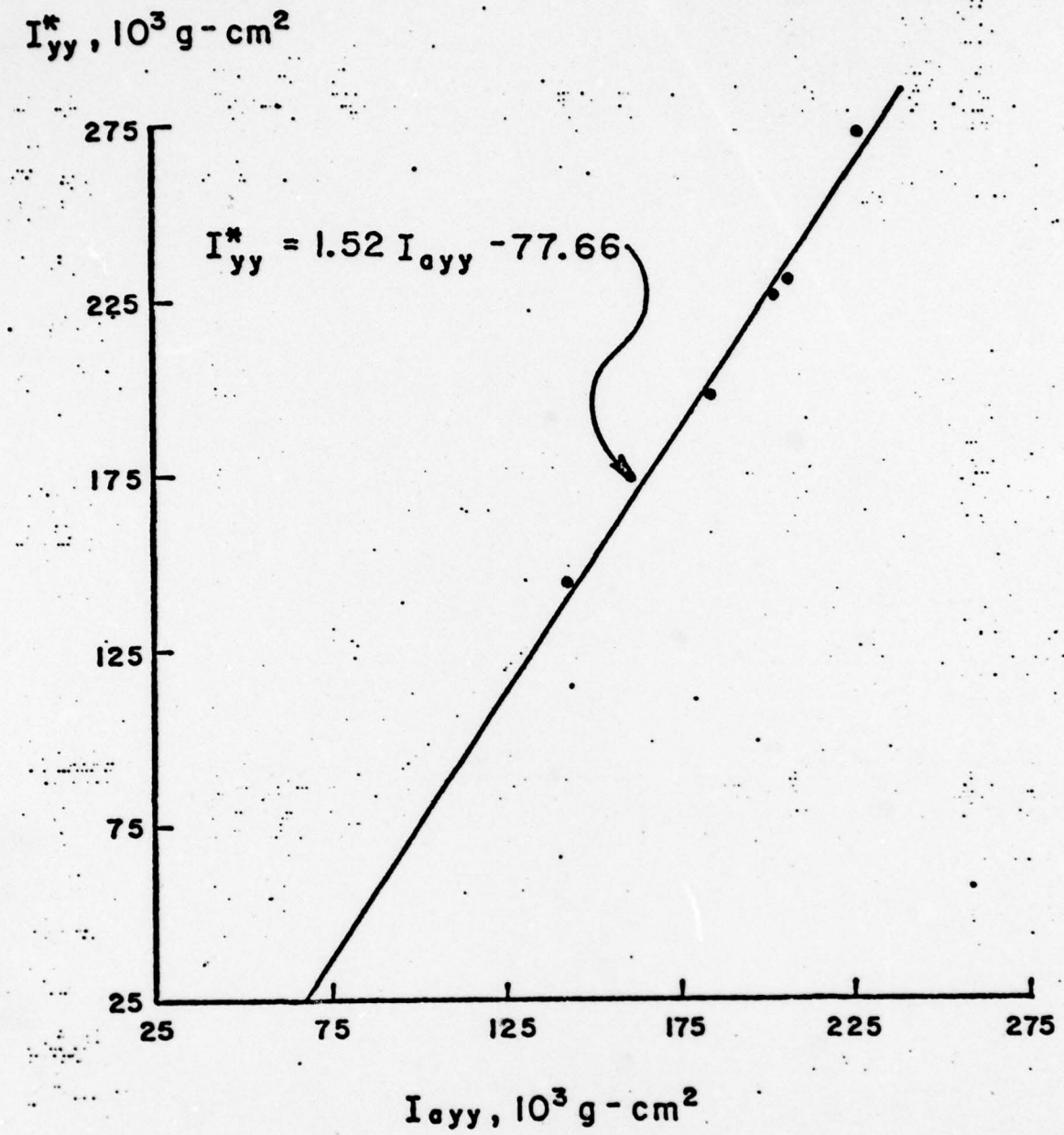


Figure 4. The Head's $I_{ayy}$ Principal Moment, Computed Using the Rotated Ellipsoid Geometric Model, Compared to the Experimentally Determined Principal Moment, $I^*_{yy}$.

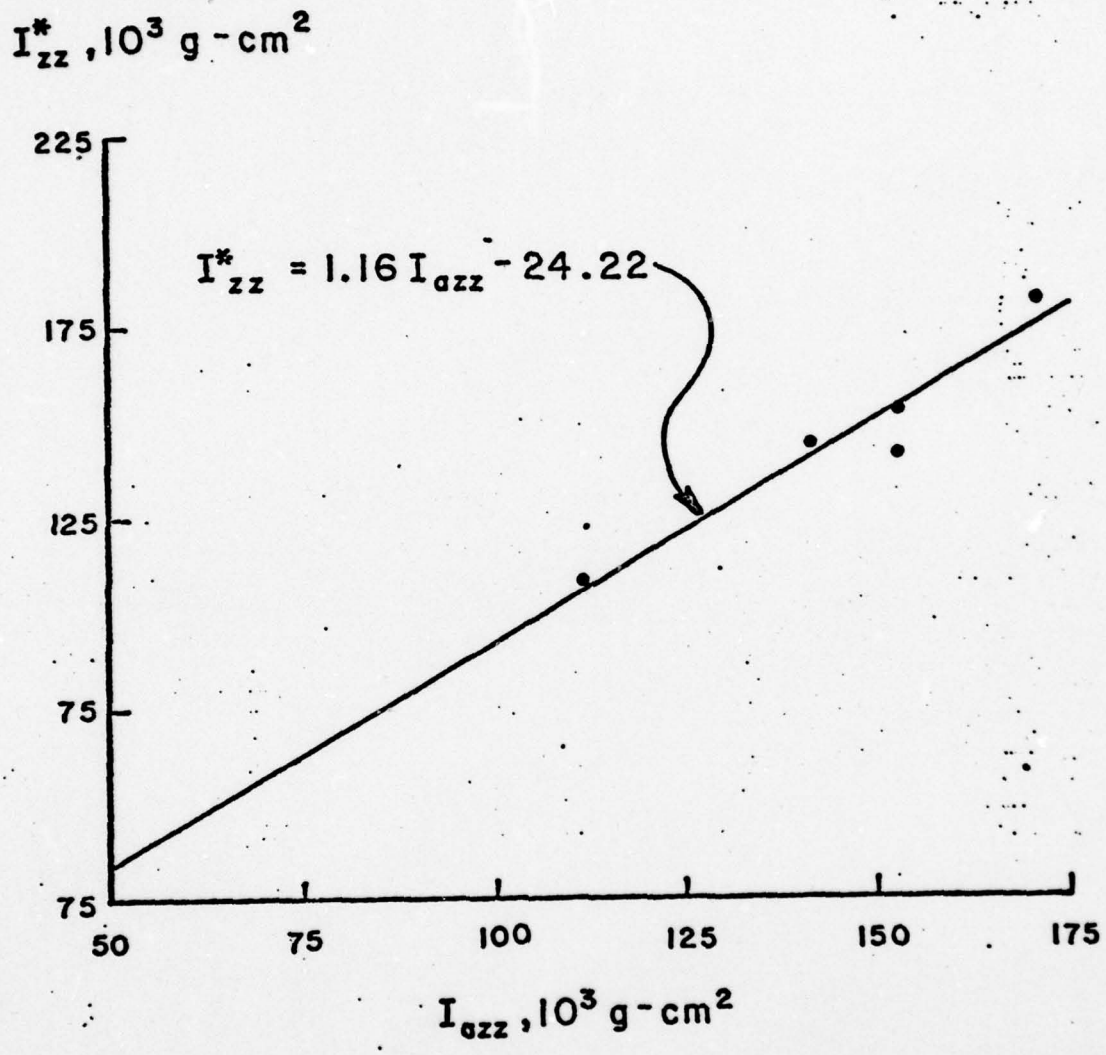


Figure 5. The $I_{azz}$ Principal Moment, Computed Using the Rotated Ellipsoid Geometric Model, Compared to the Experimentally Determined Principal Moment, $I^*_{zz}$.

The neck segment is a complex geometric shape, as shown in side view in Figure 6a. There are two cut-planes between the head and the neck: one is parallel to the Frankfort plane, passing from the back of the head along the base of the skull to a point just behind the ear; the other is parallel to the body reference y-axis and runs from the point just behind the ear (on the mastoid) tangent to the upper portion of the Adam's apple and out the front of the neck. The cut-plane between the neck and the upper torso is parallel to the body reference y-axis and passes through the vertebral landmark at the lower back of the neck called the certicale and a point just above where the two collar bones meet (the suprasternale).

The neck segment has been modeled as a three part solid: two simply-transected elliptical semicylinders with the surface curve removed on top of a right elliptical cylinder (Figure 7b). Figure 6c is a perspective view of a simply-transected elliptical semicylinder with the surface curve removed. In words, a semicylinder is a cylinder that has been bisected along its long, or z-, axis, the cut-plane being parallel to either the x- or y-axis. "Simply-transected" means that the semicylinder is cut by a plane that is parallel to the same axis as the bisecting cut-plane and runs from the bisecting cut-plane at one end-plane to the opposite side of the other cut-plane. The remaining part of the description specifies that the bisecting cut-plane is part of the solid. The part that is removed is the part containing the cylinder's surface curve.

A FORTRAN program has been written that uses the anthropometric data on the neck listed in Appendix A to compute the inertial properties of the solid with respect to a coordinate system with origin at the center of mass and axes in the same directions as the head reference system (Leet, 1978e). The program uses the inertial properties of the simply-transected elliptical semicylinder with the surface curve removed, which are summarized in Appendix C, the inertial properties of an elliptical cylinder, the parallel theorem, and some geometric relationships to determine the model's inertial properties.

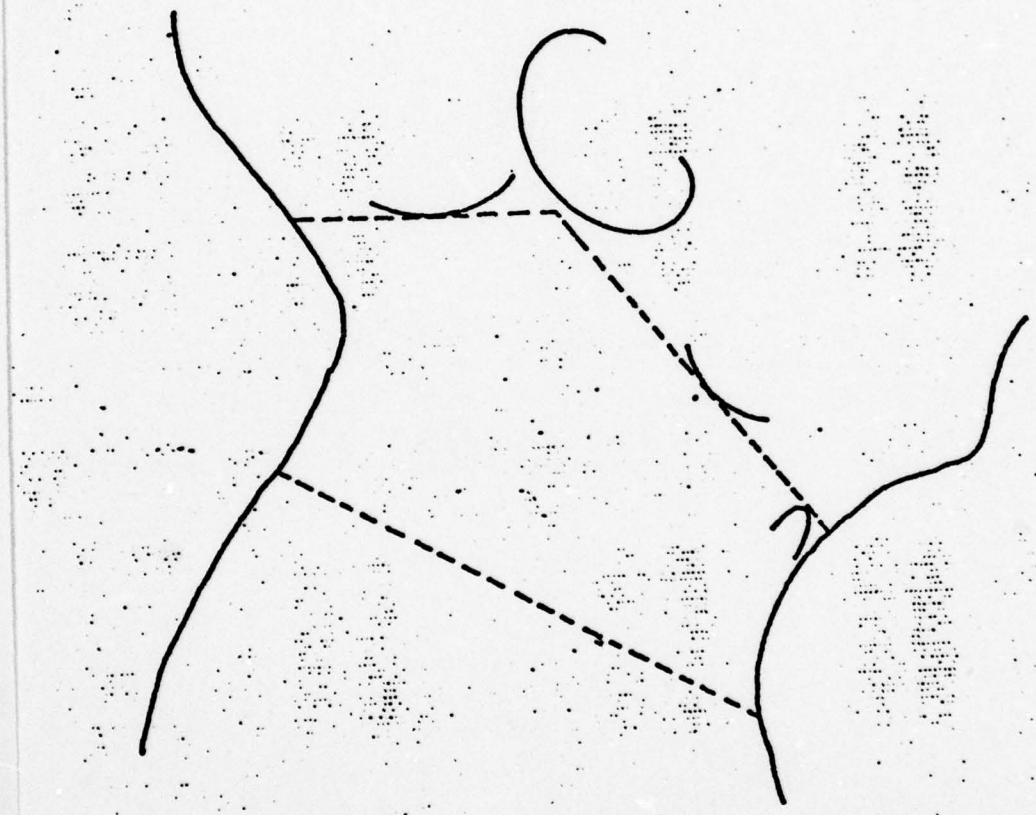

Figure 6a. Side View of the Neck Segment.

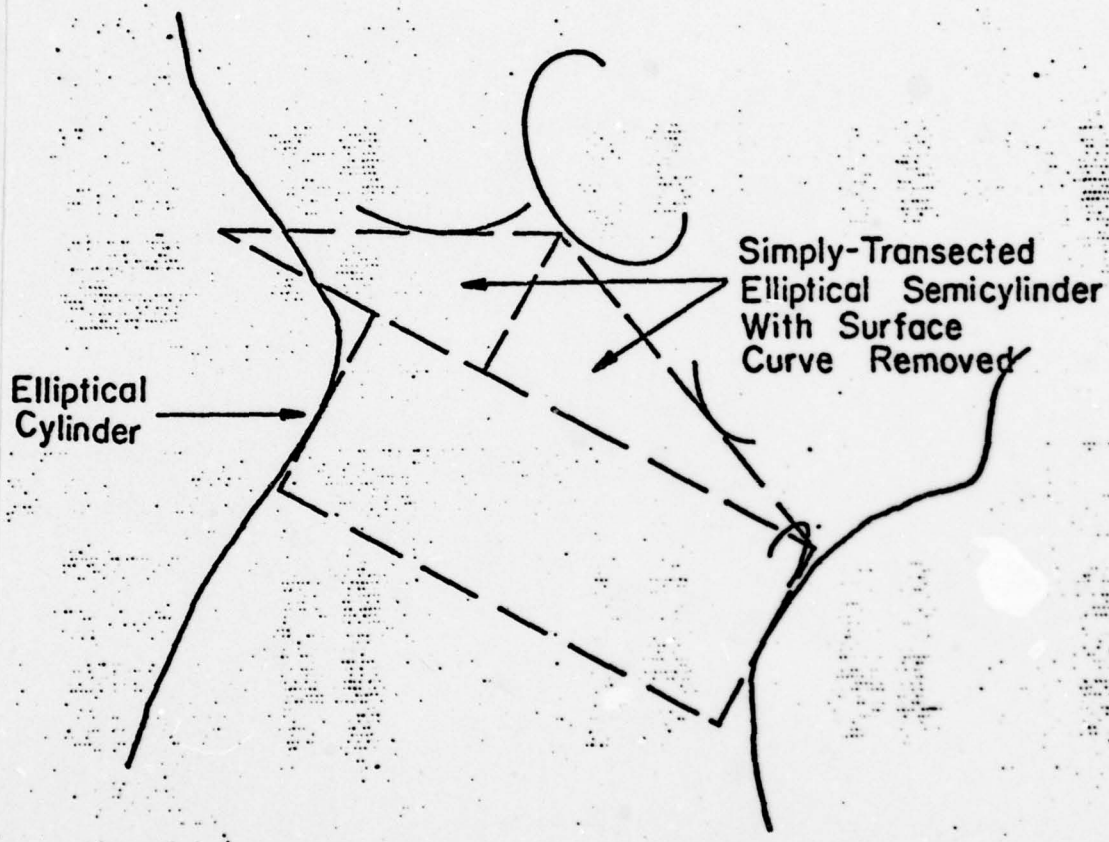


**Figure 6b. Side View of the Three-Part Neck Geometric Model.**

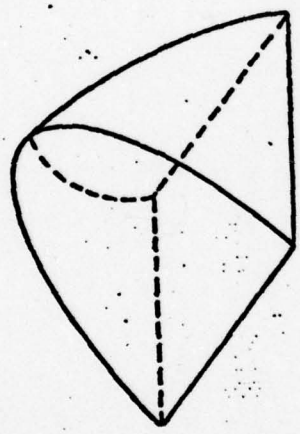

Figure 6c. Perspective View of a Simply-Transected Elliptical Semicylinder With the Surface Curve Removed.

SECTION 3

## TECHNIQUES USED TO ESTIMATE JOINT LOCATIONS

The body segments in the ATB Model are connected at joints to form the total body. The location of each segment's joints must be defined with respect to the segment's principal axes. In general, the segment's cut-planes are so defined that their centroids are the joint loci.[2] Therefore, the inertia computation process outlined above provides the necessary information to determine the joint locations. However, there are some exceptions. The head-neck joint is located at the mid-point of the line connecting the mastoids (the bone behind the ear). To locate this point with respect to the head's center of mass, anthropometric data must be available relating the center of mass to the mastoids. The neck modeling procedure provided information on the joint's location in the neck.

The neck has a second joint, the upper torso-neck joint. Assuming that it is located the same distance from the back of the neck as the head-neck joint, the coordinates of this joint in the neck can be obtained from the neck modeling procedure. The coordinates of the joint with respect to the centroid of the cut-plane between the neck and upper torso can also be determined. These coordinates can be transferred to the upper torso to provide the joint's location in the upper torso.

The shoulder joints are located using values from the upper arm and upper torso models. The joint is assumed to be one-third the distance from the top of the shoulder (acromion) to the arm pit (axilla), measured form the acromion. (This fraction is the subject of some controversy.)

The upper torso-mid torso and mid torso-lower torso joint locations are computed using a formula developed by Liu and Wickstrom (1973). With the standard local reference axis system having the

---

[2] It is recognized that there is a continuing controversy over rules that locate joints from external landmarks. This issue can not be addressed in this short summary; the results in this paper reflect the latest thinking.

positive x-axis forward, the positive y-axis to the right, and the positive z-axis down, the distance in the -x-direction from the center of mass is given by $a_0 + a_1 (W / H * Y))$, where $a_o$ and $a_1$ are regression coefficients computed by the authors for each vertebral level, W is the body weight, H is the body height, and Y is the width of the body at the joint location.

The upper torso-mid torso joint is located at about the level of the T7 vertebra. The -x-distance can be computed by averaging the values obtained from the Liu and Wickstrom formula for the T6, T7, and T8 vertebrae. The mid torso-lower torso joint is located at about the level of the L3 vertebra. The -x-distance can be computed by averaging the values obtained from the Liu and Wickstrom formula for the L3, L3, and L4 vertebrae. To complete the coordinate definitions: the y-coordinates for both points are zero; the z-coordinates can be obtained from the geometric models of the segments.

Specification of the hip joint locations requires the geometric model of the lower torso and the anthropometric measurements bispinous breadth (the point of the hip bone in the lower abdomen), which is used to compute the y-coordinate (bispinous breadth/2), the trochanterion height (the hollow on the side of the hip), which is used to compute the z-coordinate (In the geometric model calculations, the center of mass is defined with respect to the top end-plane centroid. Knowledge of the vertical distance from the end-plane, which is the iliocristale height (the very top of the hip bone), to the trochanterion is enough to define the z-coordinate.), and the trochanterion-to-seat-back distance, which is used to compute the x-coordinate.

## SECTION 4

## TECHNIQUES USED TO ESTIMATE SEGMENT CONTACT ELLIPSOIDS

The surfaces of the body model are described by the surfaces of ellipsoidal shapes for individual body segments. The present state-of-the-art provides no algorithm for generating the dimensions of these contact ellipsoids; instead, the following set of heuristics is offered. But first it should be pointed out that the segment inertia ellipsoids are independent of the contact ellipsoids. The objective of the contact ellipsoid construction is to provide a surface description for contact force interactions and to generate a representative body shape for graphic display.

The technique used is to work from side and front view photographs of a person representative of the class of individuals being modeled. The person should be in this standard sitting position: the head is oriented in the Frankfort Plane, the upper arms are vertical with the palms in, the lower arms are horizontal, the lower legs are vertical, and the feet are flat on the floor. The objective here is to position the axes of the body segments parallel to the body reference axes. The outline of the body should be clearly visible in the photographs, and scales close to the body mid-planes should be included.

The body outline and scale are traced on graph paper. The segment cut-planes are drawn on these figures, along with the segment principal axes at the center of mass. At the present time the contact ellipsoid semiaxes (The ATB Model program has the option of reorienting the contact ellipsoid semiaxes, but to date this reorientation has not been required.). The intersections of the segment principal axes with the extreme edges of the segment are used, along with a compass, to locate a first estimate of the contact ellipsoid origins. The coordinates of the origins with respect to the segment principal axes and the semiaxes lengths are supplied to the ATB Model program. This program is run for zero simulation time, followed by a body ellipsoid outline plot program

to obtain plots of the initial position of the total body in its environment. Inspection of these plots usually suggested adjustments to the contact ellipsoid dimensions or origin locations.

There is a definite "art" to these heuristics. Furthermore, the interactive process consumes a comparatively large amount of computer resources and time. Therefore, contact ellipsoid determination is a prime candidate for future procedural improvements.

# SECTION 5

## TECHNIQUES USED TO DEFINE BODY AND JOINT AXES ORIENTATION

The body orientation in the environment is defined in the ATB Model program by specifying the orientation of the segment principal axes with respect to an inertial reference system and the location of the lower torso segment's center of mass. This is a straightforward procedure.

Two coordinate systems must be defined for each joint, one in each segment associated with the joint. Their relative orientations are used to determine the torque at the joint. A manual procedure, one that sets the usual initial condition of zero joint torque has been developed and an automated approach using an interactive computer program is under development.

The required input data for this program are the direction angles of each segment with respect to the segment's local reference system and the angles of certain body segments with respect to the inertial reference system. (Generally, only one direction angle per segment is required.) The program leads the user through the required input data by asking simple, completely unambiguous questions. It generates an annotated card deck that can be used directly in the ATB Model program input data deck plus a detailed listing in the same format as is generated by the ATB Model program.

## SECTION 6
## CONCLUDING REMARKS

The obvious temptation for any programmer is to create one large interactive program that incorporates all the techniques developed so far, plus techniques that permit easy definition of the environment and contact ellipsoids, perhaps under light-pen or cursor control. Indeed, we are investigating the cost-effectiveness of such a program.

The new techniques we have described have had limited testing and use. We are hoping that publication of these techniques at this time will lead to further testing of them, along with the communication to us of any needed improvements.

Our research program will have an impact on the sciences of anthropometry and anatomy in a couple of ways. First, the geometric models we have developed require some new anthropometric measurements. We have been working closely with experts in these fields to insure that the desired measurements are practical and appropriately defined. Second, if more accurate geometric models of body segments are required, improvement will most likely be made by defining density distributions within segments. No such data currently exist.

## ACKNOWLEDGMENTS

The research reported in this paper covers work performed under contracts F33615-75-C-5054 and F33615-78-C-0504, sponsored by the 6570th Aerospace Medical Research Laboratory, Aerospace Medical Division, Air Force Systems Command, Wright-Patterson Air Force Base, Ohio. The author acknowledges the contributions of AMRL's Mr. Ints Kaleps.

## REFERENCES


1. Becker, E.B. (1973), "Measurement of Mass Distribution Parameters of Anatomical Segments", Sixteenth Stapp Car Crash Conference, Society of Automotive Engineers, Inc., New York, New York.

2. Chandler, R.E., C.E. Clauser, J.T. McConville, H.M. Reynolds, and J.W. Young (1975), "Investigation of Inertial Properties of the Human Body", AMRL-TR-74-137, Aerospace Medical Research Laboratory, Wright-Patterson Air Force Base, Ohio.

3. Fleck, J.T., F.E. Butler, and S.L. Vogel (1974), "An Improved Three-Dimensional Computer Simulation of Motor Vehicle Crash Victims, Volume I Engineering Manual, Volume II Model Validation, Volume III User's Manual, and Volume IV Programmer's Manual", Technical Report No. ZQ-5180-L-1, Calspan Corporation, Buffalo, New York.

4. Fleck, J.T. and F.E. Butler, "Development of an Improved Computer Model of the Human Body and Extremity Dynamics (1975)", AMRL-TR-75-14, Aerospace Medical Research Laboratory, Wright-Patterson Air Force Base, Ohio.

5. Leet, D.G. (1978a), "MISEC2: An Interactive FORTRAN Program That Computes the Inertia Properties of a Homogeneous Right Elliptical Solid", UDR-TR-78-26, University of Dayton Research Institute, Dayton, Ohio, 45469.

6. Leet, D.G. (1978b), "The Inertial Properties of a Simply-Transected Elliptical Cylinder", UDR-TR-78-94, University of Dayton Research Institute, Dayton, Ohio, 45469.

7. Leet, D.G. (1978c), "Estimating Moments of Inertia of the Head From Standard Anthropometric Data", UDR-TR-78-28, University of Dayton Research Institute, Dayton, Ohio, 45469.

8. Leet, D.G. (1978d), "An HP-97 Program That Computes the Inertia Properties of a Segmented, Rigid, Homogeneous Solid From the Inertia Properties of Its Parts", UDR-TR-78-29, University of Dayton Research Institute, Dayton, Ohio, 45469.

9. Leet, D.G. (1978e), "Estimating the Inertial Properties of the Neck From Anthropometric Data", UDR-TR-78-95, University of Dayton Research Institute, Dayton, Ohio, 45469.

10. Liu, Y.K. and J.K. Wickstrom (1973), "Estimation of the Inertial Property Distribution of the Human Torso From Segmented Cadaveric Data", in Perspectives in Biomedical Engineering, R.M. Kenedi (ed.), MacMillian New York, New York.

11. Reynolds, Herbert M. (1974), "Measurement of the Inertial Properties of the Segmented Savannah Baboon", Ph.D. Thesis, Southern Methodist University.

# APPENDIX A

## GEOMETRIC MODELS OF BODY SEGMENTS AND THEIR ANTHROPOMETRIC DATA REQUIREMENTS

### A.1 THE HEAD ANTHROPOMETRIC DATA

1. Head Length, hl
2. Head Depth (height), hd
3. Head Breadth, hb
4. Head, mastoid-to-vertex vertical distance, hmv
5. Head, mastoid-to-back-of-head horizontal distance, hmb
6. Head, mastoid-to-ear hole distance (x- and z-coordinates), (hmex, hmex)

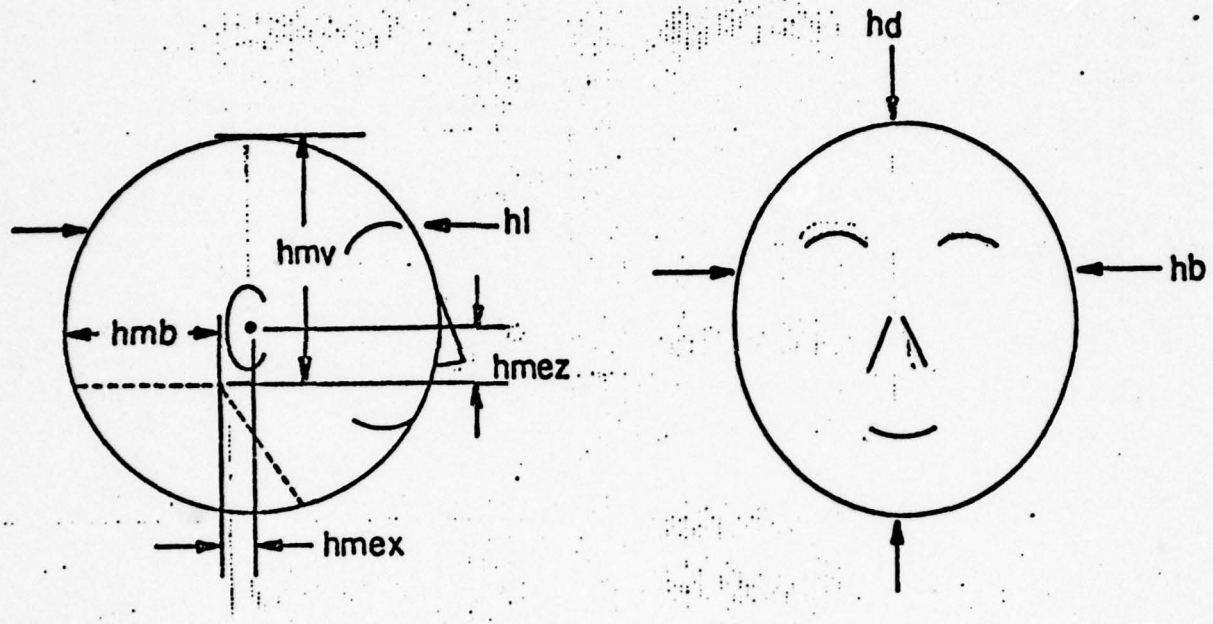


Figure A-1. The Head Segment's Anthropometric Data.

## A.2 THE NECK ANTHROPOMETRIC DATA

1. Head, mastoid-to-vertex vertical distance, nmv
2. Head, mastoid-to-back-of-head horizontal distance, nmb
3. Adam's apple-to-wall distance, nax
4. Adam's apple to vertex vertical distance, naz
5. Cervicale-to-suprasternale distance, ncs
6. Cervicale-to-Adam's apple distance, nac
7. Cervicale to mastoid distance, projection on the midsagittal plane, ncm
8. Mastoid to Adam's apple distance, projection on the midsagittal plane, nam
9. Suprasternale to Adam's apple distance, nas
10. Mid-neck depth, nd
11. Mid-neck breadth, nb
12. Mastoid-to-mastoid distance, nmm

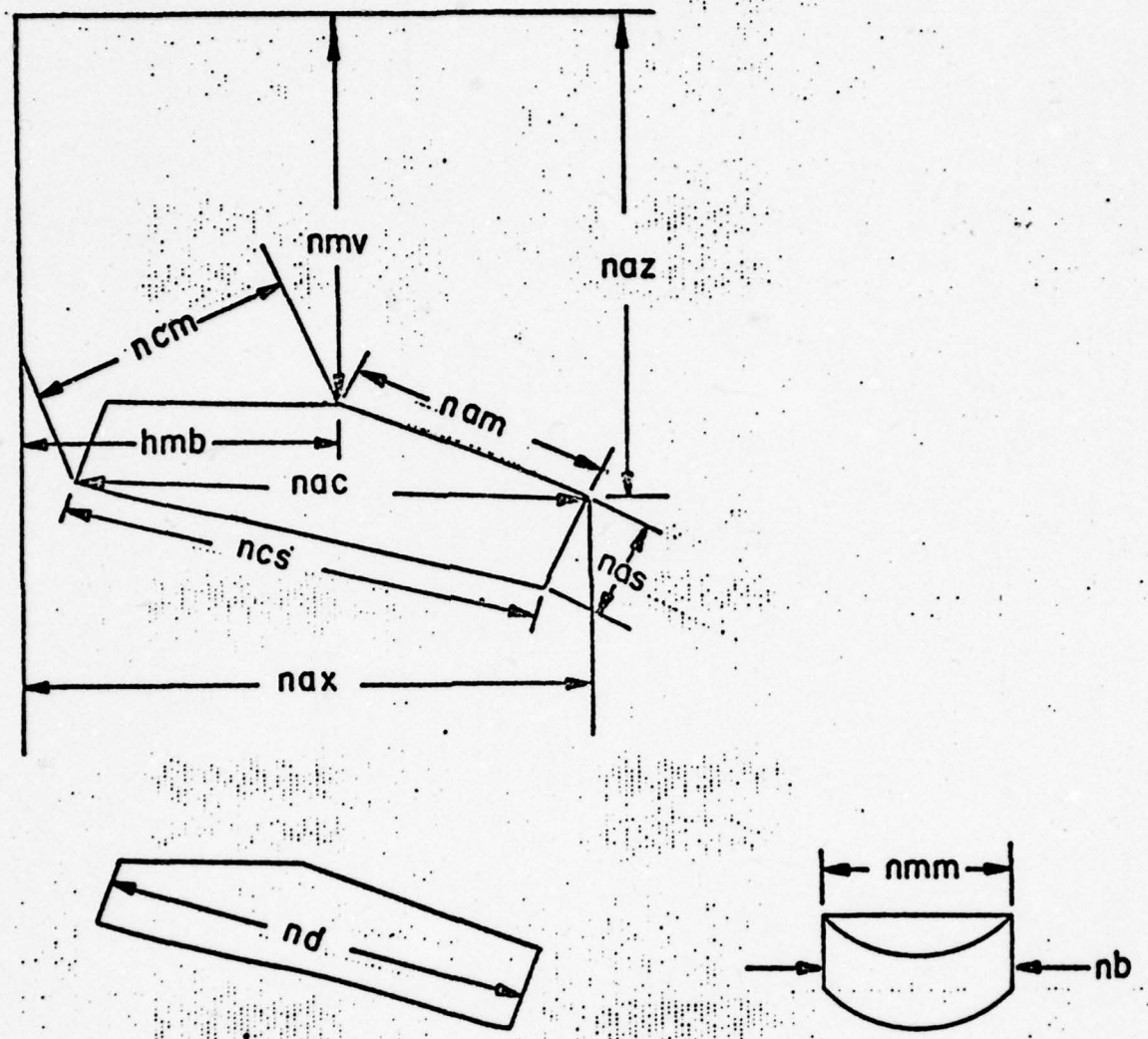


Figure A-2. The Neck Segment.

## A.3 • THE UPPER TORSO ANTHROPOMETRIC DATA

1. Biacromial Breadth, utbb
2. Horizontal depth at suprasternale, utbd
3. Depth at axilla level, utad
4. Breadth at axilla level, utab
5. Circumference at axilla level, utac
6. Depth at substernum level, utsd
7. Breadth at substernum level, utsb
8. Circumference at substernum level, utsc
9. Substernum to axilla distance, vertical, utsa
10. Substernum to acromion, vertical distance, utss
11. Volume of body to distal cut-plane of neck, utvn

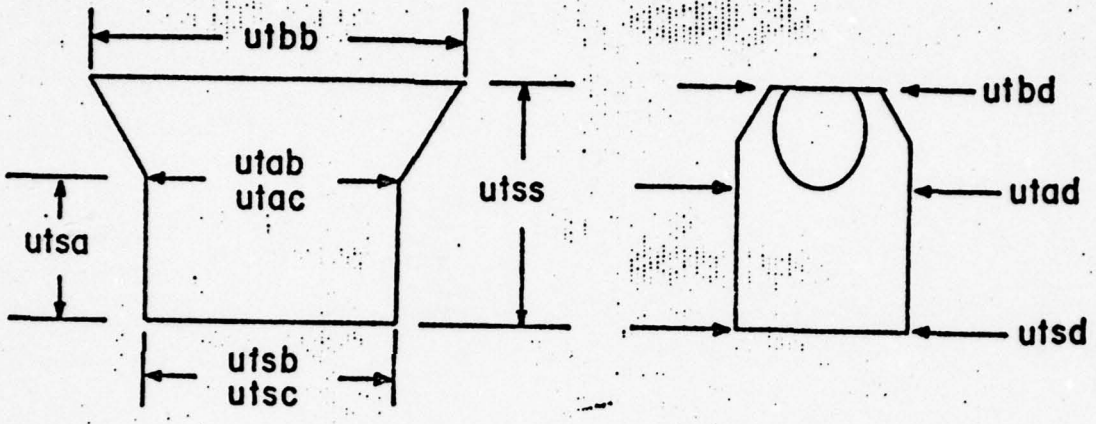


Figure A-3. The Upper Torso Segment.

## A.4 THE MIDDLE TORSO ANTHROPOMETRIC DATA

1. Substernum-to-iliocristale distance, mtsi
2. Iliocristale-to-waist (at navel) distance, mtiw
3. Depth at substernum, mtsd
4. Breadth at substernum, mtsb
5. Circumference at substernum, mtsc
6. Depth at waist (navel), mtwd
7. Breadth at waist (navel), mtwb
8. Circumference at waist (navel), mtwc
9. Depth at iliocristale level, mtid
10. Breadth at iliocristale level, mtib
11. Circumference at iliocristale level, mtic.
12. Volume from feet to substernum level,

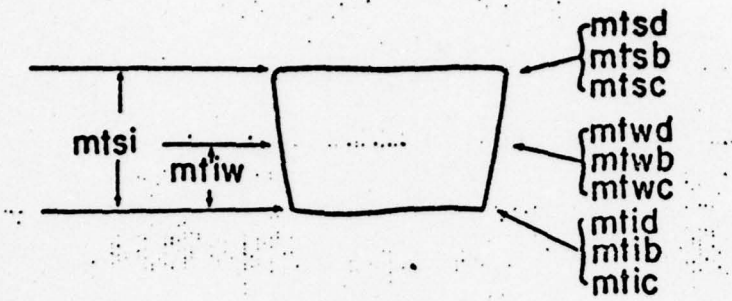


Figure A-4. The Middle Torso Segment.

## A.5 THE LOWER TORSO ANTHROPOMETRIC DATA

1. Thigh-abdominal junction height, lttj
2. Iliocristale height, ltih
3. Depth at iliocristale level, ltid
4. Breadth at iliocristale level, ltib
5. Circumference at iliocristale level, ltic
6. Depth at thigh-abdominal, junction level, lttd
7. Breadth at thigh-abdominal junction level, lttb
8. Circumference at thigh-abdominal junction level, lttc
9. Trochanterion height, ltth
10. Trochanterion-to-back distance, lttr
11. Bispineous breadth, ltbb
12. Length of the line from the thigh-abdominal junction through trochanterion to the buttock point, ltab
13. Volume from iliocristale level down, ltvd

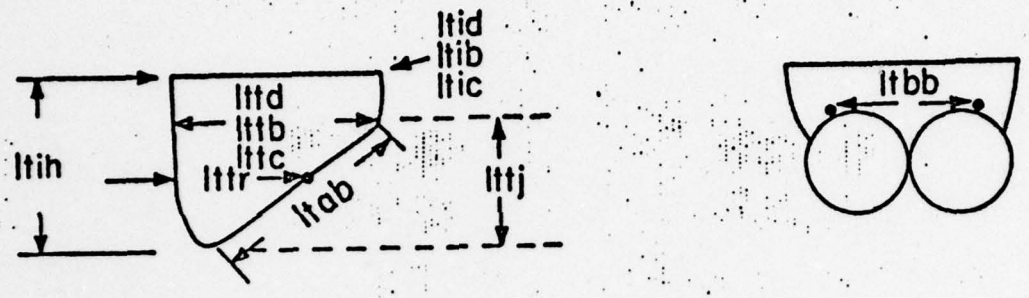


Figure A-5. The Lower Torso Segment.

## A.6 THE UPPER ARM ANTHROPOMETRIC DATA

1. Acromion-to-elbow, uaae
2. Axilla-to-elbow, uaxe
3. Depth of upper arm at level of axilla, uaad
4. Breadth of upper arm at level of axilla, uaab
5. Circumference of upper arm at level of axilla, uaac
6. Depth of upper arm midway between acromion and elbow, uamd
7. Breadth of upper arm midway between acromion and elbow, uamb
8. Circumference of upper arm midway between acromion and elbow, uamc
9. Depth of upper arm at level of lower arm-upper arm junction (inside elbow), uajd
10. Breadth of upper arm at level of lower arm-upper arm junction (inside elbow), uajb
11. Circumference of upper arm at level of lower arm-upper arm junction (inside elbow), uajc
12. Axilla-to-acromion length, uaaa
13. Breadth at elbow, uaeb
14. Circumference at elbow uaec
15. Upper arm-lower arm volume to axilla-acromion line, vual

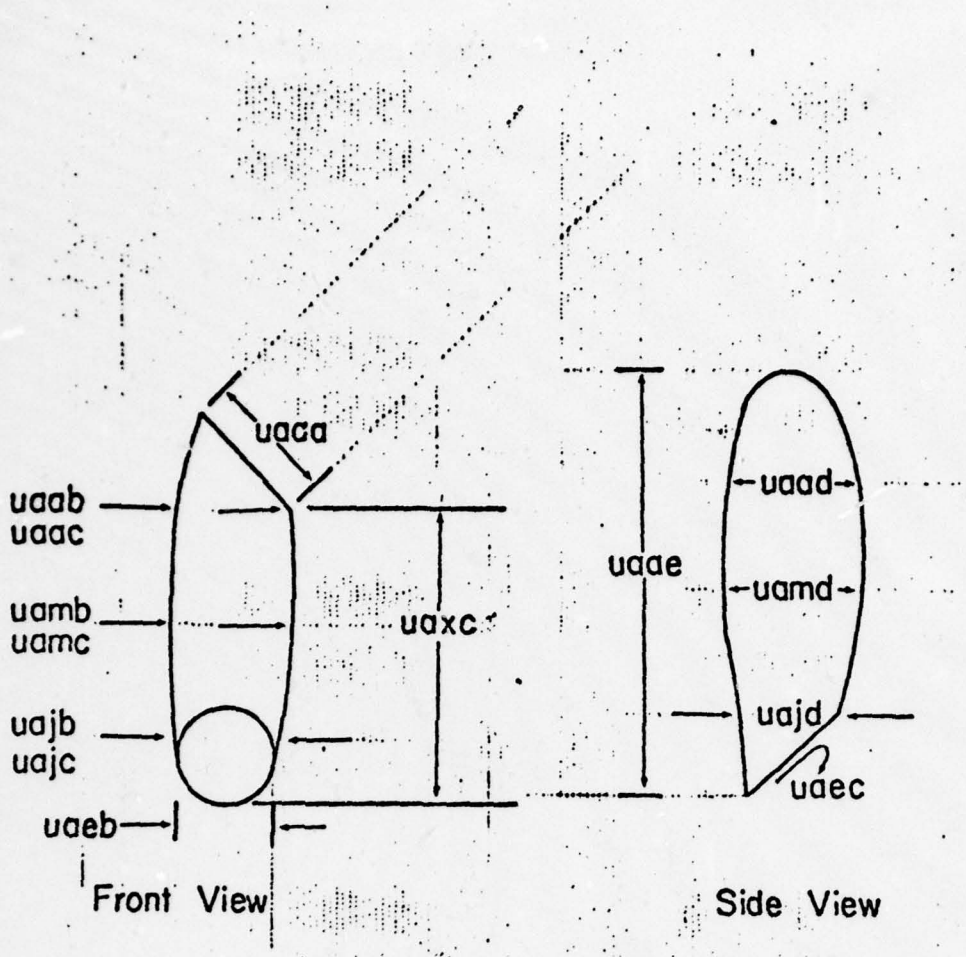


Figure A-6. The Upper Arm Segment.

## A.7 THE LOWER ARM-HAND ANTHROPOMETRIC DATA

1. Elbow-to-finger tip length, laet
2. Width of 4 fingers held tightly together, lawf
3. Depth of thickest finger at second joint, laf
4. Width of hand and thumb together, lawh
5. Maximum depth of hand, ladh
6. Depth of wrist, lawd
7. Breadth at wrist, lawb
8. Circumference at wrist, lawd
9. Hand length to wrist, lal
10. Elbow-to-wrist length, laew
11. Depth lower arm at maximum circumference, lamd
12. Breadth lower arm at maximum circumference, lamb
13. Circumference lower arm at maximum circumference, lamc
14. Elbow to lower arm maximum circumference distance, lamx
15. Depth of lower arm at arm crease, lacd
16. Breadth of lower arm at arm crease, lacb
17. Circumference of lower arm at arm crease, lacc
18. Elbow circumference, laec
19. Length of lower arm from crease to finger tip, lacf
20. Volume of lower arm-hand segment, lavh

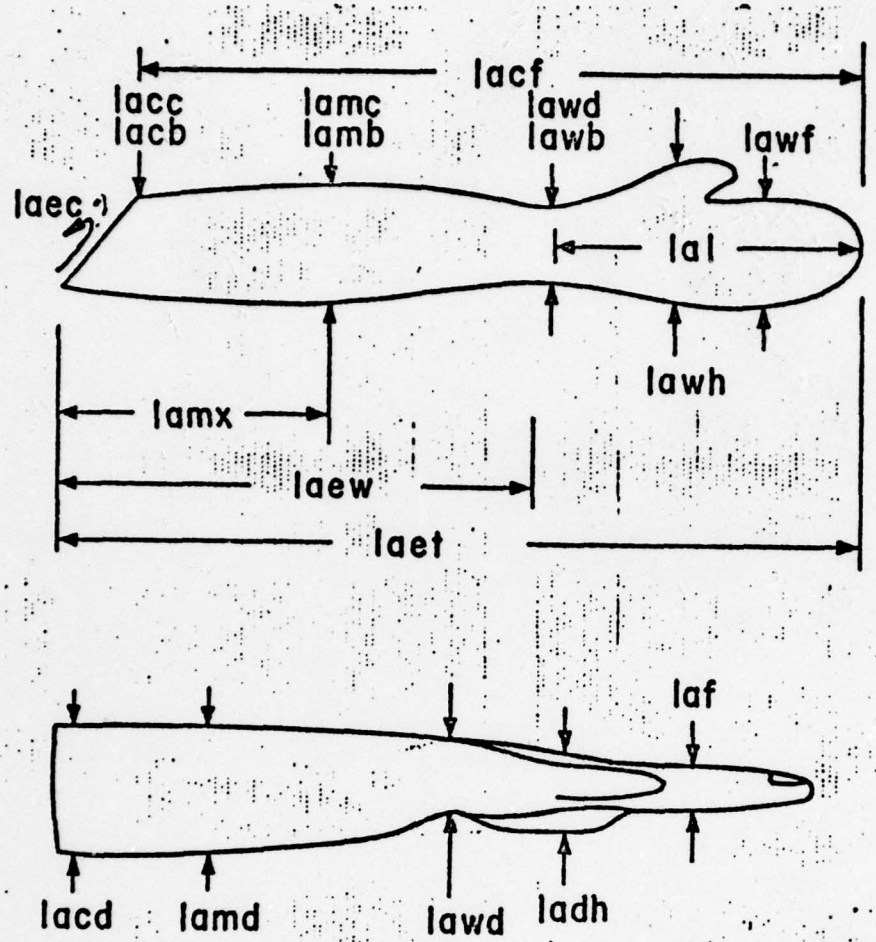


Figure A-7. The Lower Arm-Hand Segment.

1. Abdomen-thigh junction to mid kneecap distance, ulak
2. Buttocks point to crease at back of knee (The buttocks point is located by extending a line from the abdomen-thigh junction through the trochanterion point to the surface of the buttocks.), ulbk
3. Depth of leg at level of the crease at the back of the knee, ulkd
4. Breadth of leg at level of the crease at the back of the knee, ulkb
5. Circumference of leg at level of the crease at the back of the knee, ulkc
6. Depth of leg at mid-thigh, ulmd
7. Breadth of leg at mid-thigh, ulmb
8. Circumference of leg at mid-thigh, ulmc
9. Depth of leg at abdomen-thigh junction, ulad
10. Breadth of leg at abdomen-thigh junction, ulab
11. Circumference of leg at abdomen-thigh junction, ulac
12. Abdomen-thigh junction to trochanterion, ulat
13. Trochanterion to buttocks point, ultb
14. Location of mid-thigh measurements to abdomen-thigh junction, ulma
15. Volume of leg and foot (Submerge to line connecting abdomen-thigh junction and trochanterion.), lv

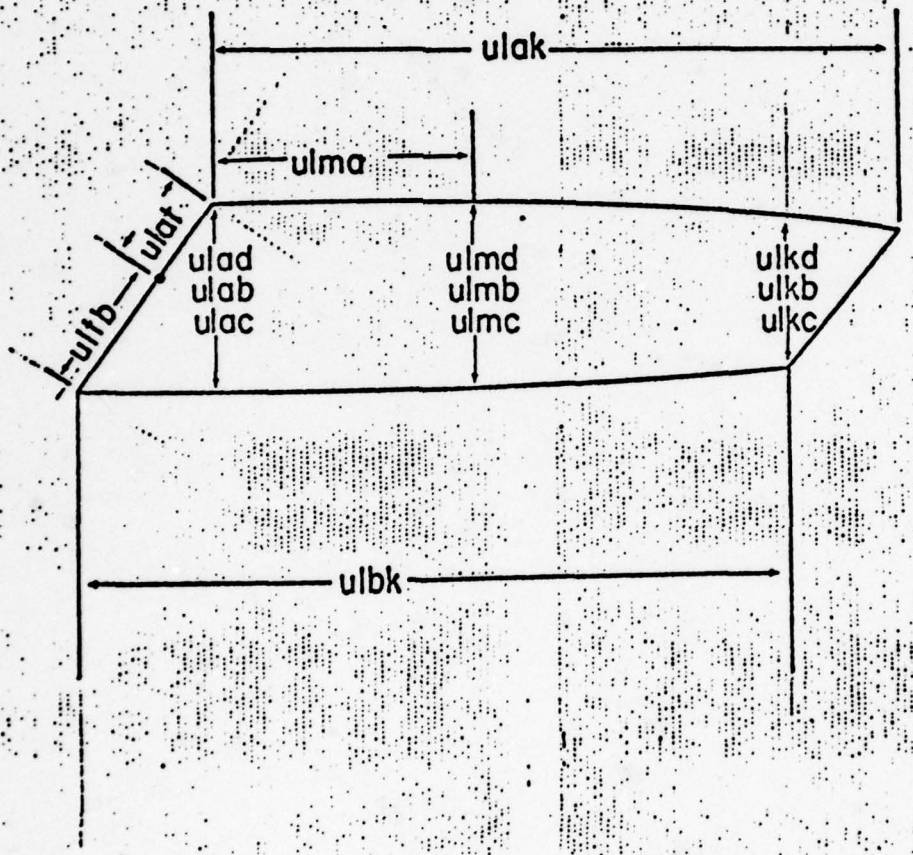


Figure A-8. The Upper Leg Segment.

## A.9 THE LOWER LEG ANTHROPOMETRIC DATA

1. Crease at back of knee to sphyrion (lower leg inside length), llli
2. Mid-kneecap to sphyrion (lower leg outside length), llo
3. Depth of leg at level of the crease at the back of the knee, llkd
4. Breadth of leg at level of the crease at the back of the knee, llkb
5. Circumference of leg at level of the crease at the back of the knee, llkc
6. Crease at the back of the knee to mid-kneecap distance, llck
7. Depth of leg at maximum calf circumference, llcd
8. Breadth of leg at maximum calf circumference, llcb
9. Circumference of leg at maximum calf circumference, llcc
10. Sphyrion to level where maximum calf circumference measurements were made, llsc
11. Depth of ankle at minimum circumference, llad
12. Breadth of ankle at minimum circumference, llab
13. Circumference of ankle at minimum circumference, llac
14. Volume of lower leg (submerge to line connecting crease at back of knee with the mid-kneecap), llv

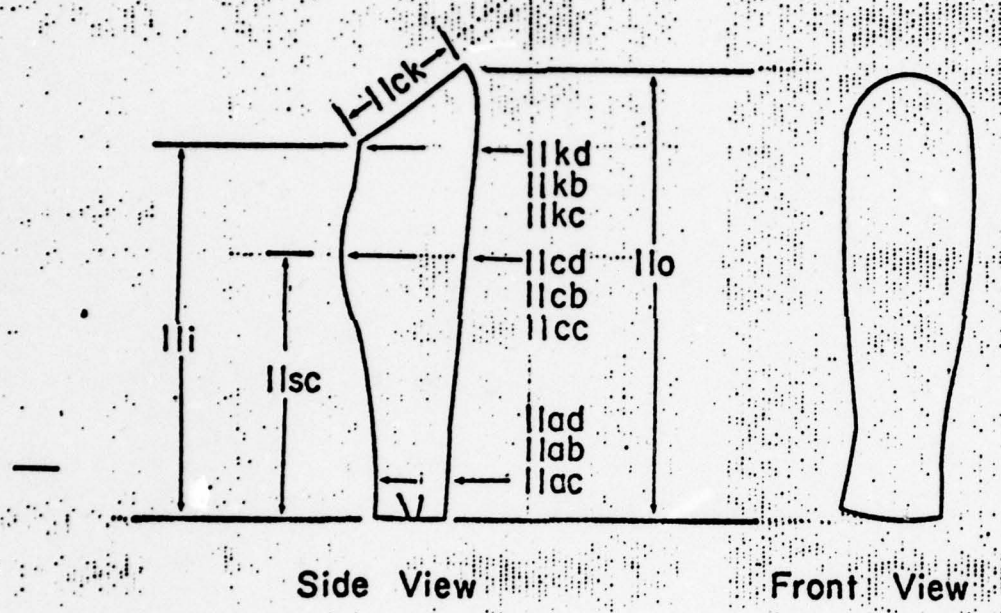


Figure A-9. The Lower Leg Segment.

## A.10 THE FOOT

1. Heel-to-toe length (maximum foot length), fl
2. Sphyrion height, fh
3. Foot height at ball of foot, fb
4. Big toe height at nail, ft
5. Distance from distal point of big toe to point where fb measurement was made, ftl
6. Width of foot at tip of toes, fwt
7. Width of foot at ball of foot, fwb
8. Width of ankle just below sphyrion, fwa
9. Volume of foot (submerged to sphyrion), fv

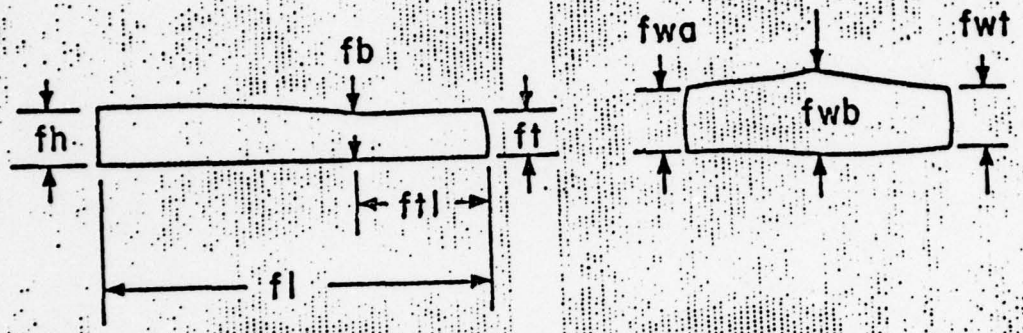


Figure A-10. The Foot Segment.

# APPENDEX B

## INERTIAL PROPERTIES OF A SIMPLY-TRANSECTED ELLIPTICAL CYLINDER

| PROPERTY | VALUE |
|---|---|
| V | $\frac{\pi}{2}abh$ |
| CMx | 0 |
| CMy | $-\frac{b}{4}$ |
| CMz | $\frac{3}{16}h$ |
| $I^*_{xx}$ | $\frac{\pi}{1536}abh(144b^2+37h^2)$ |
| $I^*_{yy}$ | $\frac{\pi}{1536}abh(192a^2+37h^2)$ |
| $I^*_{zz}$ | $\frac{\pi}{32}abh(4a^2+3b^2)$ |
| $I^*_{xy}$ | 0 |
| $I^*_{xz}$ | 0 |
| $I^*_{yz}$ | $-(\frac{1}{12}+\frac{3\pi}{128})ab^2h^2$ |

# APPENDIX C

## INERTIAL PROPERTIES OF A SIMPLY-TRANSECTED ELLIPTICAL SEMICYLINDER WITH THE SURFACE CURVE REMOVED

| PROPERTY | VALUE |
|---|---|
| Volume | $abH\left(\frac{\Pi}{2}-\frac{2}{3}\right)$ |
| CMx | 0 |
| CMy | $\frac{b}{4}\frac{(16-3\pi)}{(3\pi-4)}$ |
| CMz | $\frac{9\pi H}{8(3\pi-4)}$ |
| Ixx | $\frac{ab^3H}{2}\left(\frac{\pi}{4}-\frac{8}{15}\right)+\frac{abH^3}{3}\left(\frac{\pi}{2}-\frac{4}{15}\right)$ |
| Iyy | $\frac{a^3bH}{2}\left(\frac{\pi}{4}-\frac{4}{15}\right)+\frac{abH^3}{3}\left(\frac{\pi}{2}-\frac{4}{15}\right)$ |
| Izz | $\frac{a^3bH}{2}\left(\frac{\pi}{4}-\frac{4}{15}\right)+\frac{ab^3H}{2}\left(\frac{\pi}{4}-\frac{8}{15}\right)$ |
| Ixy | 0 |
| Ixz | 0 |
| Iyz | $-\frac{ab^2H}{5}$ |

[1] THE DENSITY IS IMPLIED IN ALL MOMENT VALUES

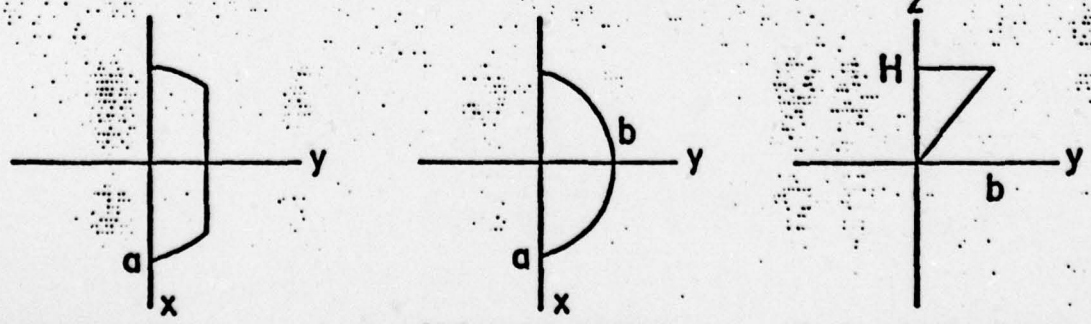


(a) SECTION (b) TOP VIEW (c) SIDE VIEW